Field Accuracy Requirements for the Undulator Systems of the X-ray FEL's at TESLA

B. Faatz, J. Pflüger

Hamburger Synchrotronstralungslabor (HASYLAB) at Deutsches Elektronen-Synchrotron (DESY), Notkestr. 85, 22607 Hamburg, Germany

Abstract

In SASE FELs, the radiation power has to saturate in a single pass through the undulator. In the VUV and X-ray regime, with undulators ranging in length from several tens to hunderds of meters, even a few percent increase in gain length could mean a lengthening of the undulator by several meters. Therefore, determining what increases the gain length is of great importance.

The influence of the electron beam quality has been studied in detail in many papers. For the TESLA X-ray FEL, with undulator lengths of up to 300 m, the gain degradation due to undulator imperfections has to be studied. Previous studies, for example for the TTF-FEL, have focused on the influence of dipole and quadrupole errors. In this report, similar results of simulations for the TESLA X-ray FEL undulators will be presented. In addition, other sources of errors, mainly related to the multi-segmented character of the undulators, will be discussed and upper limits will be given.

1. Introduction

The TESLA X-ray FEL facility is a proposed user facility in the wavelength range between 0.85 Å and 6 nm. The longest wavelength is equal to the shortest wavelength produced by the TESLA Test Facility (TTF) FEL, under construction at DESY [1]. Similar to the TTF-FEL, the TESLA X-ray FEL is an FEL that employs the principle of Self Amplified Spontaneous Emission (SASE), in which the radiation is built up from the shotnoise produced by the electron beam in a single pass through the undulator. This scheme is used because no high reflectivity mirrors are available in this wavelength range.

The layout of the X-ray FEL is shown in Fig. 1. The electron beam produced by the accelerator will have an energy between 15 and 30 GeV, distributed over two beam lines, one in the energy range from 15 to 25 GeV, a second one between 20 and 30 GeV. After the beam is collimated both in energy and size, a fast kicker at the end of both beamlines will make it possible to distribute the electron beam to two undulator beam lines each, i.e. four lines in total (see Fig. 1). For each energy, one undulator has a fixed gap, the second has a variable gap. The wavelength to be generated in the fixed gap device determines the electron beam energy, whereas the wavelenth in the second undulator is tuned by choosing the appropriate gap. Therefore, both users can have an independently

X-FEL facility layout

tunable, 200-1000 keV

U2

tunable, helical 80-100 keV

U1

optics1 — exp1

optics2 — exp2

optics3 — exp3

SASE1

1,5-5,0/1,0-3,5/1-2,5 Å tunable, planar

20/25/30 GeV

SASE2

1,3/0,85/- Å fixed gap, planar

option

U3

tunable, 20-80 keV

optics4 — exp4

optics5 — exp5

70 · 100 · 370 · 390 · 400 · 420 · 440 · 460 · 470 · 490 · 510 · 520 · 540 · 760 · 800

SASE5

10-58/4-25 Å tunable, helical

optics6 — exp6

optics7 — exp7

SASE3

2,4/1 Å fixed gap, planar

15/(23)25 GeV

SASE4

3,0-10,0/1-3,5 Å tunable

U4

tunable, 10-30 keV

U5

tunable, 10-30 keV

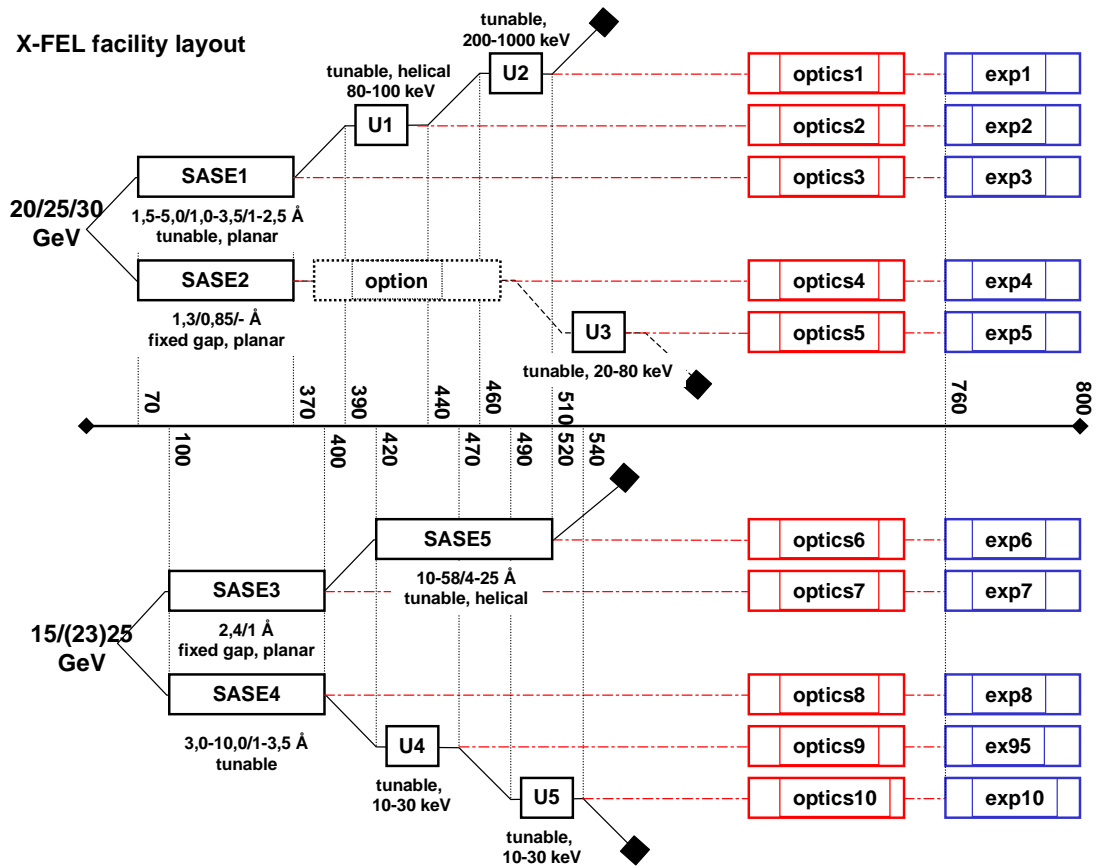optics8 — exp8

optics9 — ex95

optics10 — exp10

Fig. 1. Schematic layout of the TESLA X-ray FEL facility. The facility consists of four planar undulators in the short wavelength range (0.85 to 10Å) , one helical undulator at longer wavelengths (4 to 58 Å) and five spontaneous radiators. The future optional extension for a two-stage FEL to reduce the bandwidth is already shown.

tunable wavelength at their disposal. While the electron beam produces the SASE FEL radiation, its energy reduces due to emission of synchrotron radiation. At the same time, the energy spread increases. Therefore, the beam can no longer be used to generate SASE radiation at the same wavelength. At longer wavelengths, however, it is still possible to produce intense SASE light. In addition, broadband spontaneous radiation, which does not suffer from reduced beam quality, can also be produced. Therefore, behind one undulator beamline (SASE-3), a second undulator is placed to produce SASE radiation at a longer wavelength (SASE-5), behind three (SASE-1, SASE-2 and SASE-4), spontaneous radiators are placed. Behind SASE-2, there is space reserved for a so-called two-stage FEL option. This principle allows to narrow the FEL radiation bandwidth without reducing the output power, thus increasing the spectral brilliance by close to three orders of magnitude [2].

Each undulator system with a total length of several hundred meters, consists of cells. Each cell is built up of an undulator segment, phase shifters to match the phase between segments of electrons and radiation field, and a quadrupole in a FODO structure to keep the beam at a constant small diameter.

Because saturation has to be reached in a single pass, the electron beam has to be of high quality. This means that both transverse emittance and energy spread have to be small. Especially the normalized emittance of $1.6\,\pi$ mm mrad is a challenge, since this value is at the limit of what has been achieved so far. Furthermore, because the peak currents needed for the FEL cannot be achieved for any existing electron source, the beam has to be longitudinally compressed and transversely focused. For the beam parameters given in Table 1, the saturation

Electron beam energy, $\mathcal{E}$	13 – 50 GeV
Peak current, I	5.0 kA
rms bunch length	25 μm
rms transverse beam size at 25GeV	38 μm
rms normalized slice emittance, ϵ_n	1.6 mm mrad
rms energy spread, σ_E	2.5 MeV
Macropulse duration	1070 μs
Bunch separation	93 ns
Number of pulses per train	11500
Repetition rate	5 Hz

Table 1
Electron beam parameters at the entrance of the TESLA X-ray FEL undulators

length, and thus the minimum undulator length, has been calculated both analytically and with the use of simulation codes [3–5]. These simulations assume, however, that the electron beam is perfectly matched to the undulator optics and the undulator is ideal. In practice, components can be misaligned, the magnetic field is not perfect and the beam has some random variation of initial condictions, such as position, angle and energy. All these effects will reduce the gain and therefore increase the required undulator length.

In this report, the influence of undulator imperfections on the gain degradation is studied. The remainder of this report is organized as follows. In Sec. 2, the different sources of undulator errors are discussed. Sec. 3 briefly discusses the simulation code that has been used to simulate the FEL process. Sec. 4 describes the results of simulations of statistical errors caused by random peak field errors and quadrupole misalignment. In Sec. 5, the results are summarized and conclusions are drawn as to what errors play the main role.

2. Different sources of undulator errors

The sources of undulator errors can be grouped in different ways. One classification would be to distinguish between local and global errors. Local errors are short range, in many cases of statistical nature, and their influence is usually determined by performing many simulations with random distributions of for example rms field errors, quadrupole misalignment, etc. Long range errors, typically on the scale of a gain length, are for example misalignment of entire undulator modules, different on-axis values for K-parameter (or undulator gap), etc. In case of the TESLA X-ray FEL, the field gain length for 1Å is about 20 m, which is longer than 4 undulator cells. In this report, we therefore distinguish between steering and non-steering errors. Steering errors reduce the (transverse) overlap between electron beam and radiation field, whereas non-steering errors destroy the phase relation between field and beam without changing their overlap. For the TTF-FEL, this has been studied in Refs. [6,7]. The different error sources are the following:

(1) Non-steering errors

    (a) Difference in K-value (or gap) of undulator segments
    (b) Phase matching between undulator segments
    (c) Misplacement of undulator segments

(2) Steering errors

    (a) Variation in (dipole) field strength and direction
    (b) Variation in quadrupole position and strength

In most cases, steering errors also give a non-steering contribution and vice versa, for example undulator field variation.

3

The influence of some of the above mentioned parameters, such as undulator peak field variation, depends on the exact distribution of the magnets used (see for the TTF-FEL parameters Refs. [6,7]). Therefore, this effect can only be treated either if the real distribution is known or by using statistical methods. Because the real distribution is known only after the magnets have been produced and measured, only statistical procedures can be used before the undulator is built. The next section shows results of such statistical procedures.

Many so-called global variations are related to the resonance condition and an upper limit can be given without performing the actual simulations. The resonance condition is given in one dimension (plane wave) by

$$\lambda = \frac{\lambda_{\mathrm{u}}}{2\gamma^2}(1 + K_{rms}^2)\,, \tag{1}$$

where λ_{u} is the undulator period, γ is the electron beam energy normalized the electron rest mass (Lorentz factor) and $K_{rms} \approx 93 B_{\mathrm{u}}[\mathrm{T}] \cdot \lambda_{\mathrm{u}}[\mathrm{m}]$ is the rms value of the undulator strength with B_{u} the on-axis rms undulator field strength. For a sinusoidal field, $K_{rms} = K_{peak}/\sqrt{2}$. With an rms spectral bandwidth of a SASE FEL of the order of ρ (see for example Ref. [8]), the K_{rms} parameter between undulator segments has to be constant within (see also Ref. [9])

$$\frac{\Delta\lambda}{\lambda} = \frac{2K_{rms}\Delta K_{rms}}{1 + K_{rms}^2} \approx \frac{2\Delta K_{rms}}{K_{rms}} < \rho\,, \tag{2}$$

where the latter approximation is valid for large K_{rms}-values. The natural FEL bandwidth thus gives an upper limit on tolerable K_{rms}-parameter variation. If this value would vary more between segments, the amplification process would use the bunching that has developed before, but not the field. Hence, a second frequency spike would develop next to the main one. For any fixed gap device, K_{rms} has to be constant within these margins. For a variable gap device, such as the TESLA FEL undulators, the tolerances within which the gap has to be adjusted can be estimated using Hallbachs' approximation of the field. For a NdFeB-type undulator, the on-axis magnetic field B_{u}, which is proportional to K_{rms} is given by

$$B_{\mathrm{u}} = 3.694 \times e^{-5.068 g/\lambda_{\mathrm{u}} + 1.52(g/\lambda_{\mathrm{u}})^2} \quad \rightarrow \quad \frac{\Delta g}{g} \times \left[-5.068\frac{g}{\lambda_{\mathrm{u}}} + 3.04\left(\frac{g}{\lambda_{\mathrm{u}}}\right)^2\right] \approx \frac{\Delta B_{\mathrm{u}}}{B_{\mathrm{u}}} < \frac{\rho}{2}\,, \tag{3}$$

with g the undulator gap. The value for ρ changes with radiation wavelength and with electron beam energy. As a safe lower limit for the reproducebility of the gap, one can choose $2\Delta K_{rms}/K_{rms} = 2\Delta B_{\mathrm{u}}/B_{\mathrm{u}} \approx \rho \approx 4 \cdot 10^{-4}$ for a typical SASE X-ray FEL. This results in a gap that has to be constant within approximately $2\,\mu$m, which is an achievable goal.

The phase slippage between undulator segments can be treated in a similar way. Inside the undulator, the electrons have a transverse velocity component induced by the undulator magnetic field. Therefore, the electrons slip backwards with respect to the SASE radiation by a wavelength while the radiation travels the distance of one undulator period. Consequently, the electrons and radiation field remain in resonance along the entire undulator. Between undulator segments, this relation is broken because there the field is zero. In order to start the amplification process coherently once entering the next segment, the electrons have to slip backwards an integer number of radiation wavelengths. In the time a photon travels the distance between undulator segments L_D, an electron travels a distance $L_D \cdot v_z/c = L_D \cdot \beta_z$. Therefore, if

$$L_D(1 - \beta_z) = n\lambda\,, \tag{4}$$

with n an arbitrary integer, there is constructive interference. If the electron beam has no transverse velocity component, i.e. $\beta_z = \beta \approx 1 - 1/(2\gamma^2)$, this can be written (using Eq. (1)) as

$$L_D = n\lambda_u(1 + K_{rms}^2)\,. \tag{5}$$

4

For any fixed gap undulator, which has a constant K_{rms}-value, the distance is therefore fixed, i.e. independent of the choosen electron energy. For the TESLA X-ray FEL, with K-values between 3.7 and 7 and undulator periods of 45 or 60 mm, this would result in a minimal distance of the order of 0.8 meter. For a variable gap device, one cannot maintain resonance between segments unless an additional delay is introduced using a three magnet chicane, also called a phase shifter. Such a device is described in Ref. [10]. In this case, including the transverse kick, the relation becomes

$$L_D(1 + (\gamma x')^2) = n\lambda_u(1 + K_{rms}^2) \quad \text{with } \gamma x' = \frac{e}{mc}I_1, \tag{6}$$

where $I_1 = \int B dz$ is the integral of the dipole field applied, typically of the order of a few T mm. Simulations of multi-segmented undulators performed for the TTF-FEL have shown that the phase between segments does not have to be matched very accurately [11]. A phase mismatch as large as 20 degrees does not significantly decrease the gain.

Another point is the positioning of undulator segments. Since there is no focusing in the horizontal direction, an offset in the x-direction does not change the undulator field strength. An offset in y, in which the undulator has some weak focusing, the offset can also be rather large. The variation of K_{rms} is proportional to $\cosh(k_u y) \approx 1 + \frac{1}{2}(k_u y)^2$, with $k_u = 2\pi/\lambda_u$ is the undulator wavenumber (see Ref. [9]). Comparing the change in K_{rms}-value due to a shifted undulator again with the ρ-parameter results in

$$\frac{2\Delta K_{rms}}{K_{rms}} \approx (k_u y)^2 < \rho \rightarrow y < 200\,\mu\text{m}, \tag{7}$$

where an undulator period of 60 mm has been assumed (see also Ref. [9]). This value is indeed a lower limit, because in practice, the electron beam will perform a betatron oscillation, focusing it back to the undulator axis. An angular displacement, which would result in a different undulator period seen by the electrons of $\lambda_u/\cos(\phi)$, where ϕ is the angle under which the undulator is placed, is even more relaxed. The angle $\phi^2 < 2\rho$, which is approximately 30 mrad, is easily achieved. Further effects of the modular setup of the undulator on the FEL performance, such as diffraction and loss of phase coherence in the intersections don't decrease the gain, as shown in [12,13]. The influence of debunching in the quadrupoles placed in the intersections is discussed in [14]. In order to keep the magnetic field strength constant in time, temperature stabilization has to be provided. With a reversible temperature coefficient of NdFeB of 0.11%/$^{\circ}C$, the temperature has to remain constant within $\pm 0.2\,^{\circ}C$ [9].

The previous analytical estimates on tolerances have shown that the most demanding one is the accuracy with which the undulator gap can be determined. All these estimates, however, assume that the undulators themselves are manufactured perfectly. In addition, the quadrupoles are assumed to be perfectly aligned. In order to determine their influence, simulations have been performed for many different distributions of magnets with different errors.

3.   Error model used in the simulation code Genesis 1.3

The simulation code Genesis 1.3 is described in Ref. [5]. Here, we will only recall the main features before discussing the treatment of errors in more detail. The code Genesis 1.3 solves the electron and wave equations in the paraxial, approximation. The wave equation is expended on a Cartesian grid. Equations are averaged over an undulator period, with the exception of the error term in the undulator field. An external FODO lattice is taken into account without a smooth approximation.

Due to error terms in Genesis, only those equations describing the transverse electron dynamics have been altered. In all other equations, the modified transverse coordinates and momenta have been used to calculate the change in longitudinal electron dynamics and evolution of the radiation field. The differential equations of the transverse coordinate are

$$x' = \frac{p_x}{\gamma}, \quad p_x' = -\frac{K_{rms}^2}{\gamma}k_x^2 x \pm \frac{e}{mc}Q(x + x_Q) + \frac{e}{mc}\delta B_u(z)\cos k_u z, \tag{12a}$$

Table 2

Parameters of the TESLA X-ray FEL for which the simulations have been performed, corresponding to the SASE-1 undulator tuned to a radiation wavelength of 1 Å for a beam energy of 25 GeV.

Electron beam	
Energy	25 GeV
Peak current	5 kA
Normalized rms emittance	1.6π mm mrad
rms energy spread	0.01 %
External β-function	45 m
rms beam size in the undulator	38 μm
Undulator	
Type	Hybrid, Planar
Period length	60 mm
Peak magnetic field	0.67 T
Magnetic gap	22 mm
Undulator segment length	5.04 m
FODO-lattice	
Period	12.24 m
Quadrupole length	0.20 m
Quadrupole strength	27 T/m

$$y' = \frac{p_y}{\gamma}, \quad p'_y = -\frac{K^2_{rms}}{\gamma}k^2_y y \mp \frac{e}{mc}Q(y+y_Q), \tag{12b}$$

where we have used, for convenience, the high-γ approximation. The undulator vector potential is approximated by $K^2(x,y) = (1 + k_x^2 x^2 + k_y^2 y^2)K^2_{rms}$, which is averaged over an undulator period, where K_{rms} is the undulator parameter including error term and $k_x^2 + k_y^2 = k_u^2$. For a helical undulator, $k_x = k_y$, for a planar, $k_x \approx 0$. Furthermore, $p_x = P_x/mc$ and $p_y = P_y/mc$ are the normalized canonical momenta, x_Q and y_Q represent the displacement of a quadrupole with strength Q in the x and y-direction, respectively. All other parameters have been defined in Sec. 2. The canonical momentum does not include the undulator error term. Hence, the differential equation for p_x shows an explicit dependence on δB_u. This term does not appear in the equation for x', because it cancels with the explicit undulator term, of which the ideal part cancels after averaging. The error term δB_u is a piece-wise constant function, varying from half-period to half-period. As can be seen from the equations, the error term is described by a single parameter. As a consequence, only peak field errors can be described. Because all errors are more or less equivalent, describing only peak field errors is sufficient.

In all calculations performed for this study, we have assumed $k_x = 0$ and $k_y = k_u$, which means that we do not take into account the defocusing of the planar undulator in the wiggle plane. This condition can always fulfilled with a sufficient width of the undulators. Misalignment of the quadrupoles in the y-direction, as described by y_Q, is also not considered. Since it is independent of misalignment in the x-direction, and basically has the same effect, results due to both misalignments will be larger by a factor of $\sqrt{2}$.

4. Results of simulations

The TESLA X-ray FEL parameters used for the simulations presented in this section are given in Table 2. These values correspond to the SASE-1 undulator tuned to a radiation wavelength of 1Å for an electron beam energy of 25 GeV. The SASE-1 undulator has been choosen because it is the most critical one. It has the largest gain length. Other undulators (SASE-2 and SASE-5) have been simulated at their minimum wavelength, giving equivalent results.

Since one can, in principle, always correct for steering errors resulting from a non-zero field integral, the first set
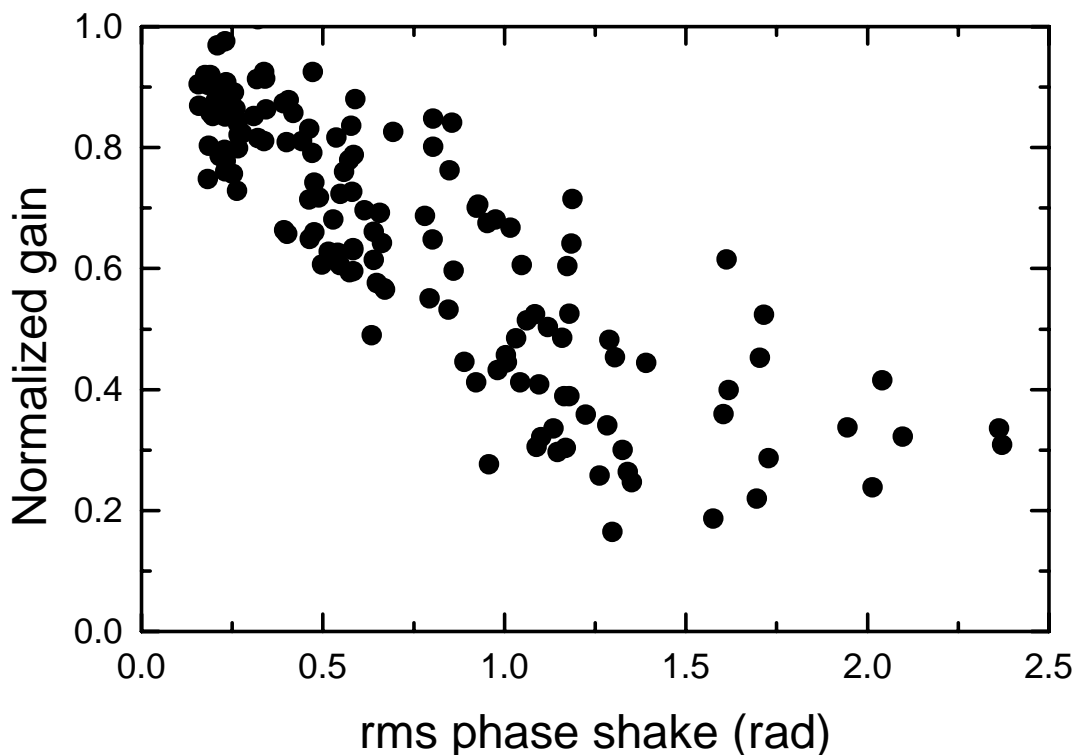
Fig. 2. The gain compared to that for an ideal undulator due to random dipole errors. Errors are random per udulator period, keeping the electron beam close to the undulator axis. Parameters used for the simulation are given in Table 2.

of simulations is done keeping the beam on axis. This can be achieved by generating period errors. In this model the K-parameter varies from period to period, thus keeping the first field integral zero. In Fig. 2, the gain, normalized to the gain of a perfect undulator, versus rms phase-shake (see Sec. 2) is shown for a beam energy of 25 GeV. The results are consistent with simulations performed by other authors (see for example Ref. [15,16]). Straight forward calculations show that as long as $\psi_{rms} < \sigma_\gamma / (\gamma \rho \sqrt{3})$, with ρ the Pierce parameter (see Ref. [8]), the gain reduction is small compared to the reduction due to energy spread. This results in an upper limit of 0.3 radians for the rms phase-shake, which is an achievable goal. Values larger than this reduces the gain significantly, as confirmed by the simulation results.

Results in Fig. 2 give an estimate on the phase-shake that is allowed, but the error distribution used is not very realistic. In a more realistic situation, the non-zero first and second field integrals will result in wander of the electron beam, thus reducing the overlap between amplified wave and electron beam. For this reason, the following simulations have been performed with a magnetic field error per half period. In Fig. 3 the gain for a 25 GeV electron beam is shown as a function of beam wander for an rms field error of 0.1%. Compared to the previous figure, where the same error gave a reduction in gain of no more than 15 %, one can see that the influence of the beam wander causes the gain to be reduced to almost zero in some cases. This is not only a consequence of the reduced overlap of electron beam and radiated wave, but also due to that fact that a collective transverse momentum results in a locally different resonance wavelength, i.e., in an additional phase-shake. Because the main effect is the beam wander in this case, the gain reduction is given versus this parameter, rather than versus phase shake (see also Ref. [7]).

In an earlier study of the influence of gain reduction for the TTF-FEL, it has been shown that if the second field integral is corrected, either by shimming or by corrector stations, the gain reduction still follows the same curve. Hence, correcting the field integral, thus reducing the beam wander, will automatically result in an increase in gain
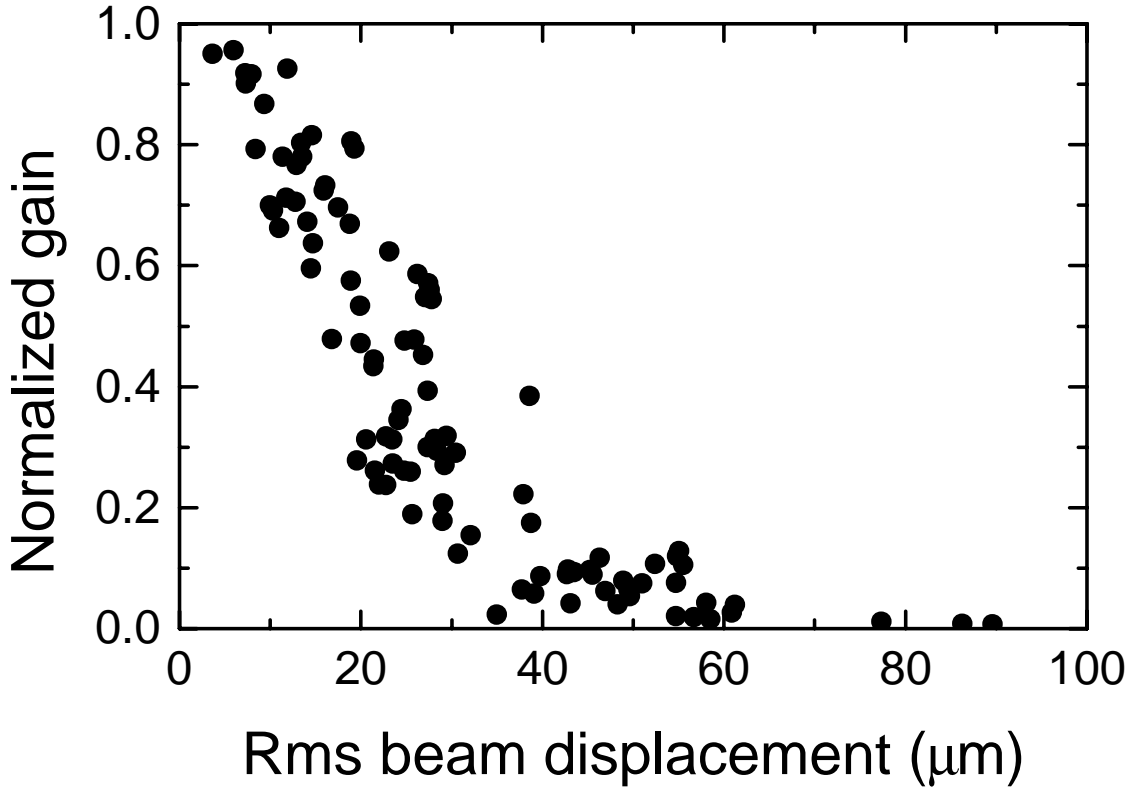
Fig. 3. *The gain compared to that for an ideal undulator as a function of rms electron beam wander at 25 GeV for the SASE-1 undulator tuned to a radiation wavelength of 1 Å. Calculations have been performed for a perfectly aligned FODO-structure. All remaining parameters are as in Table 2.*

(assuming that the phase shake plays a minor role, which is the case for the field parameters used). A separate study on alignment of the electron beam for the TTF-FEL has shown that if one uses one steerer per (power) gain length, the electron beam orbit is close to ideal. According to Fig. 3, the rms beam wander has to be smaller than $7\,\mu m$. Using $\gamma mc \cdot x = e \int \mathrm{d}z' \int \mathrm{d}z'' B(z'')$, this value corresponds to 550 T mm^2 for the second field integral on axis, i.e., not including the possible effects of the FODO lattice. One should be aware that beam wander is calculated from an integral along a particle trajectory, whereas a field integral is performed along a straight line, i.e. one-dimensional.

For the TESLA X-ray FEL, with its separated FODO lattice, a random misalignment of the different quadrupoles gives an additional component to the beam wander. Fig. 4 shows results of simulations with a displacement of quadrupoles up to $\pm10\mu$m. One can easily see that the results look similar to those presented in Fig. 3. The quadrupole offset of 1 μm is rather small, but a beam based alignment study of the TESLA X-ray FEL undulator has shown that this value can be achieved [17].

5. Discussion and Conclusions

Calculations have been performed assuming the parameters as given in Tables 1 and 2. Magnetic undulator errors result, independent of their source, in either phase shake and/or to beam wander. Phase shake is the random variation of the resonance condition, i.e. the phase between electron beam and optical wave. Electron beam wander
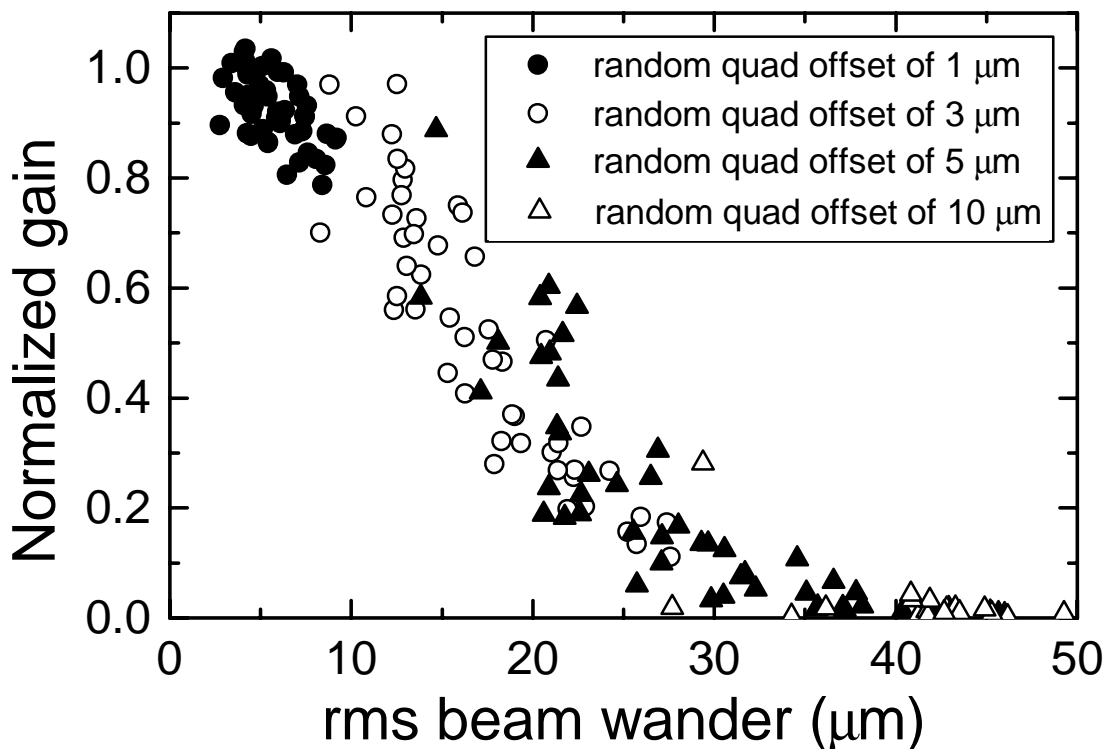
Fig. 4. Gain reduction due to quadrupole misalignment. The undulator field is assumed to be ideal. All other parameters are as in Table 2.

is the deviation of the beam trajectory from its ideal path along the optical and magnetic axis. In order to determine what tolerances are acceptable for different error sources, one can look at all of them separately.

The kick produced by variation of the undulator period is equivalent to a kick by peak field errors if $\Delta\lambda_u/\lambda_u = \Delta K_{rms}/K_{rms}$. The influence of magnetization direction errors is equivalent to peak field errors if the angle deviation $\phi \approx 2\Delta K_{rms}/K_{rms}$. Therefore, describing peak field errors or one of the two other errors gives similar results. Since they all are statistical in nature, they all contribute indepently to both beam wander and phase shake.

Simulations of peak field errors have shown that the undulator tolerances for the TESLA X-ray FEL are mainly related to the transverse overlap of the radiation field with the electron beam and the phase-shake related to this beam wander. The phase-shake for an on-axis electron beam turns out achievable, as was shown by simulations of errors per period (Fig. 2), thus fixing the electron beam to the undulator axis. Straight forward calculations show that as long as $\psi_{rms} < \sigma_\gamma/(\gamma\rho\sqrt{3})$, with ρ the Pierce parameter (see Ref. [8]), the gain reduction is small compared to the reduction due to energy spread.

The error per half period reduces the overlap between electron beam and radiation field. For an rms field error smaller than 0.1%, the reduction in gain turns out to be anything between a few percent and almost 100 % (see 3). The amount of reduction depends on the first and second field integral, related to the beam wander and phase shake. If one adds a random displacement of quadrupoles, the conclusions are virtually the same. For a displacement smaller than $\pm 1~\mu$m, the gain reduction for the 25 GeV beam is less than 15%, for displacement larger than this value the gain reduction is usually larger, as shown in Fig. 4. The simulations show that the rms value of the electron beam wander should not exceed 0.2 σ_{beam}. The beam wander scales inversely proportional with the energy. For 25 GeV a $7\mu m$ rms beam wander (corresponding to $0.2\sigma_b$ for a β of 45 m) corresponds to a second field integral of 550 T mm^2.

In case the desired first and second field integrals with the associated beam wander and phase shake can not

be achieved, the electron trajectory can be aligned with the radiation field by steering stations. The minimum number of stations is determined by the possibility to recover the maximum gain, i.e., the gain in case there are no undulator errors, and the maximum possible strength of the individual stations. The total number of steering stations is approximately equal to one per gain length, with one additional one for matching at each undulator module entrance. For the TESLA X-ray FEL, a horizontal and vertical corrector is foreseen for every quadrupole, i.e. every 5 m. With a power gain length of approximately 10 m at 25 GeV for a radiation wavelength of 1Å, this is more than sufficient to keep the beam on axis.

The simulations of which the results are shown use statistical methods, resulting in upper limits on values for phase shake and beam wander. Because they are of statistical nature, however, they do not include correction that are made after an undulator segment is assembled. In reality, the actual field is far from being statistical. The field is measured and corrected. Two methods to improve the undulator quality considerably are shimming [18,19] and pole height adjustment [20]. Similar to correcting the beam with the aid of correctors, both methods ensure that one moves along the curves shown in Figs. 2 to 4 to smaller phase shake and beam wander. Unlike correction with steerers, however, correction of the magnetic field is performed locally at the position where the error occurs and therefore much more efficient.

References

[1] *"A VUV Free Electron Laser at the TESLA Test Facility: Conceptual Design Report"*, DESY Print TESLA-FEL 95-03, Hamburg, DESY, 1995

[2] J. Feldhaus et al., Opt. Commun. **140**, (1997) 341.

[3] E.L. Saldin, E.A. Schneidmiller, M.V. Yurkov, *The Physics of Free Electron Lasers*, Springer, Berlin-Heidelberg (2000) and references therein.

[4] E. L. Saldin, E. A. Schneidmiller, and M. V. Yurkov, Nucl. Instrum. and Methods A**429**, (1999) 233.

[5] S. Reiche, Nucl. Instrum. and Methods A**429**, (1999) 243.

[6] B. Faatz, J. Pflüger and P. Pierini, Nucl. Instrum. and Methods A**375**, (1996) 441.

[7] B. Faatz, J. Pflüger and Y.M. Nikitina, Nucl. Instrum. and Methods A**393**, (1997) 380.

[8] R. Bonifacio, C. Pellegrini and L.M. Narducci, *Opt. Commun.* **53** (1985) 197.

[9] M. Rüter, J. Pflüger *"Conceptual design of the gap separation drives for the undulators for the TESLA X-FEL"*, TESLA-FEL 2000-07, DESY (2000)

[10] J. Pflüger, M. Tischer, *"A Prototype Phase Shifter for the Undulator Systems at the TESLA X-ray FELs"*, TESLA-FEL 2000-08, DESY (2000)

[11] B. Faatz, J. Pflüger, Y. Nikitina *Geometrical Undulator Tolerances for the VUV-FEL at the TESLA Test Facility*, TESLA-FEL report TESLA-FEL 96-13, Hamburg, Germany.

[12] K.-J. Kim, M. Xie, C. Pellegrini, Nucl. Instrum. and Methods A**375**, (1996) 314.

[13] K.-J. Kim, *Undulator Interruption in Huigh-Gain Free Electron Lasers*, LBNL-40689 report (1997).

[14] B. Faatz, *"Influence of different focusing solutions for the TESLA X-ray FEL's on debunching of the electron beam "*, TESLA-FEL 2000-15, DESY (2000)

[15] B.L. Bobbs, G. Rakowsky, P. Kennedy, R.A. Cover and D.Slater, *Nucl. Instr. Meth.* **296** (1990) 574

[16] Richard P. Walker, *Interference Effects in Undulator and Wiggler Radiation Sources* Sincrotrone Trieste ST/M-93/3, (1993)

[17] B. Faatz, P. Castro, *"Beam Based Alignment of the TESLA X-ray FEL undulator"*, TESLA-FEL 2001-04, DESY (2001)

[18] J. Chavanne, P. Elleaume, Synchrotron Radiation News, **8** (1995) 18

[19] I. Vasserman and E.R. Moog, Rev. Sci. Instr, **66** (1995) 1943

[20] J. Pflüger, H. Lu, T. Teichmann, Nucl. Instr. and Methods A**429** (1999) 386